ELSEVIER

Journal of Power Sources 86 (2000) 261–268

JOURNAL OF POWER SOURCES

www.elsevier.com/locate/jpowsour

The impinging jet flow cell — a novel method for the study of PEM fuel cell material

U. Koponen [a], T. Peltonen [b], M. Bergelin [a], T. Mennola [c], M. Valkiainen [b], J. Kaskimies [c], M. Wasberg [a,*]

[a] *Åbo Akademi, Laboratory of Inorganic Chemistry, Biskopsgatan 8, FIN-20500 Åbo, Finland*
[b] *VTT Chemical Technology, Otakaari 3A, FIN-02044 VTT, Finland*
[c] *Helsinki University of Technology, Advanced Energy Systems, POB 2200, FIN-02015 HUT, Finland*

Accepted 24 November 1999

Abstract

The electrocatalytic properties of a fuel cell catalyst ink in thin film form based on Vulcan XC72/Pt (30%) and Nafion was investigated by means of a flow cell of impinging jet type in flows of H_2 and H_2 + CO dissolved in H_2SO_4 electrolyte. CO adlayers of different coverages were produced by a dosing procedure and their electrooxidative removal was studied. Ru was deposited onto the ink in situ by electroreduction and the basic voltammetry of such electrodes was investigated as well as the influence on CO adlayers and CO-tolerance. A Nafion film on top of the ink film influenced both the behaviour of CO adlayers and CO-tolerance. The feasibility of the flow cell for investigation and modification of ink electrodes were demonstrated.

Keywords: Impinging jet; Flow cell; Fuel cell catalyst; Ru-modification; CO-tolerance

1. Introduction

The systematic study of the electrocatalytic properties of PEM fuel cell electrodes is a complicated and time consuming process if made in situ in assembled fuel cells. In order to reduce experimental time and to simplify data interpretation carbon supported catalyst inks have been used in single cells in the form of thin films [1–9]. Some of the catalyst inks [7–9] were also deposited on rotating electrodes to make use of the hydrodynamic capabilities of RDE systems. In the course of the development of membrane electrode assemblies in cooperation between the laboratories, the question of a rapid evaluation method for catalyst ink became of interest; it was decided to investigate the possibilities of a flow cell approach. Thus, a flow cell of impinging jet type was developed, in which the electrolyte-dissolved fuel or catalyst modifier can be directed onto the ink electrode surface to be studied. The flow composition is conveniently selected by changing flow channels by means of a computer controlled rotating valve. A similar system was earlier used in electrocatalytic studies on large surface area electrodes [10,11] and on smooth [12] and single crystal Pt electrodes [13,14]. The flow cell approach has several advantages compared to using cells with static electrolyte, for example, accurate control of chemical composition of electrode environment, controlled dosing of catalyst and reaction modifier/interfering substance, and the possibility to continuously supply fresh reactant to and remove reaction products from the electrode under study. On the one hand, previous experience with the behaviour of CO [12–14] and the deposition of Ru on smooth Pt electrodes [15,16] made it natural to look at in situ Ru modification of the catalyst ink and the adsorption and oxidation of mono and submonolayers of CO dosed onto the ink in a controlled way. On the other hand, attention to the behaviour of CO on fuel cell relevant ink electrodes is important since CO deactivation still remains a large problem to be overcome for reformed hydrogen [17] and direct methanol fuel cell anodes [18]. In addition, the usefulness of the flow system on longer time scales in the study of CO poisoning during amperometric hydrogen oxidation has been demonstrated.

2. Experimental

A gold electrode of 1.7 mm diameter housed in PTFE teflon was used as a substrate for an ink based on Vulcan

* Corresponding author.

0378-7753/00/$ - see front matter
PII: S0378-7753(99)00497-8

XC-72 (Pt 30%) from E-TEK and Nafion. A piece of adhesive tape with a hole of 1.7 mm diameter was attached on top of the working electrode, leaving only the gold surface free, before spin-coating the ink in three steps, followed by drying of the ink under an IR-lamp. The mass of the ink was in the range 20–50 μg, corresponding to a Pt loading of 100–300 μg cm^{-2}. This ink electrode was used as prepared or after modification by electrochemical Ru deposition. A Nafion film was also deposited onto some of these electrodes by spin-coating using a 5% Nafion solution (E-TEK). The electrodes were characterized in 0.5 M H_2SO_4 (Merck, suprapur, Millipore MilliQ water). Ru deposition was accomplished from a 3 mM $RuCl_3$ solution (Sigma) in 0.5 M H_2SO_4 electrolyte. Hydrogen oxidation was achieved using a flow of H_2SO_4 electrolyte through which hydrogen gas (Alfax AB 99.9996%) was sparged. For CO-tolerance measurements, a flow of 1.4% by volume CO gas (Linde 99.95%) bled into the hydrogen gas. CO dosing experiments were made with electrolyte sparged with pure CO gas. The flow cell was a three-compartment cell with reversible hydrogen electrodes as reference and counter electrodes and has been described earlier in detail [12]. The main difference compared to the earlier work with bead type electrodes was that the working electrode was now completely immersed into the bulk electrolyte. The flow of electrolyte was directed onto it through a silica capillary tube that entered the cell at the bottom. The excess electrolyte was removed from the cell by using a peristaltic pump. The flow in the cell was propelled by hydrostatic pressure: the height difference between the electrolyte level in the cell and the containers, respectively, was ca. 80 cm. Depending on experiments, two or three flow channels were used and the desired flow was selected by using a computer controlled rotating valve (Omnifit). Since the inner diameter of the capillary tube (0.5 mm) was smaller than that of the working electrode, a flow of wall-jet type was expected [19]. Consequently, a plot of the limiting current for oxidation of H_2 at different flow rates vs. $v^{3/4}$ resulted in a straight line. The flow rate was approximately 0.30 ml min^{-1} and all experiments were made at room temperature. The current densities given are with respect to the geometric area of the ink electrode unless otherwise stated.

3. Results

3.1. Basic voltammetry of pure ink

The electrode potential for each ink electrode was, after immersion, first cycled between 0.05 and 0.7 V. The voltammograms became stable after ca. six cycles but the hydrogen peaks of the Pt crystallites were not well-defined (curve A in Fig. 1). When the potential was swept up to 1.5 V, some fine structure in the hydrogen peaks appeared. An increase in the active Pt area could also be noted as a result of the sweep to 1.5 V. This is an indication that impurities are present in the ink and that electrooxidation and reduction of the ink had a cleansing effect. In order to avoid surface structural changes in the crystallites, these extended potential excursions were kept to a minimum.

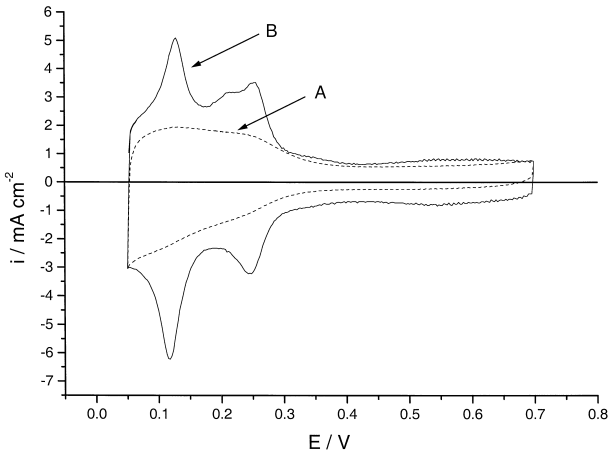

Fig. 1. Comparison of basic voltammograms in the hydrogen and double layer region for the pure ink electrode before CO dosing and stripping (A) and after (B), in 0.5 M H_2SO_4 electrolyte flow. Scan rate: 0.05 V s^{-1}.

The flow system allows controlled dosing of dissolved adsorbing molecules such as CO. After such a dosing was undertaken and the adsorbed CO was oxidized away in pure H_2SO_4 electrolyte flow, a very well-defined hydrogen voltammogram was obtained (curve B in Fig. 1). Apparently the effect of the strongly adsorbing CO was to expel the impurities from the Pt surface. The well-defined voltammograms were stable throughout the rest of the measurements made on a particular film, which indicates that impurities originated from the ink.

The contribution of Pt(110) and Pt(100) surfaces, peaks at ca. 0.12 and 0.25 V, are clearly observed in the hydrogen voltammogram for the CO-cleansed surface. In fact, the voltammetry resembles very closely that obtained by Schmidt et al. [8], although they, in their electrode treatment, first deposited the carbon supported catalyst and then covered it with a Nafion film. The hydrogen desorption charge, obtained by current integration between 0.05 and 0.4 V and corrected for capacitive charge, for the electrode used in Fig. 1 was ca. 270 μC, which gives a real Pt surface area of ca. 1.4 cm^2 for the electrode, assuming that 200 μC; this charge is consumed per square centimeter surface Pt. The mass of this particular ink was not determined but was found to be on an average 35 μg. This corresponds to a theoretical surface Pt area of ca. 5 cm^2. Thus, less than half of the total Pt surface was accessible to the electrolyte in our studies.

3.2. Ru modification by in situ electrodeposition

In situ Ru deposition was carried out in steps by electroreduction at 0.1 V using a flow channel containing

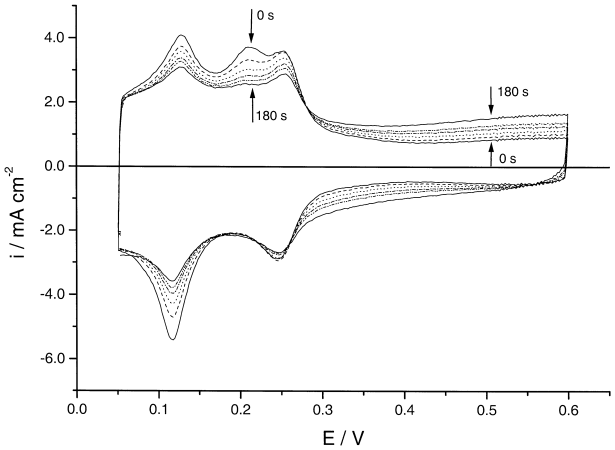

Fig. 2. Effect of in situ Ru electrodepostion on basic voltammetry in 0.5 M H_2SO_4. Ru was deposited in steps at 0.1 V in a flow of $RuCl_3$ containing electrolyte (3 mM Ru) for 0, 10, 20, 30, 30 and 90 s. Scan rate: 0.05 V s^{-1}.

Ru solution. After each Ru dosing step, a CV sweep was made in the potential range 0.05–0.6 V. Fig. 2 shows the resulting CVs together with a base voltammogram for the pure catalyst film after Ru doses of 0, 10, 20, 30, 30 and 90 s duration. A total dosing time of 180 s was thus achieved. The major change in the voltammetry was a continuous decrease in the hydrogen electrosorption activity and an increased double layer charging response. The decrease in peak height for the peaks at 0.12 V, assigned to Pt(110)-like sites, is a continuos function of total deposition time. The same is true for the decrease in oxidation peaks at 0.2 and 0.25 V, Pt(100)-like sites. This indicates that Ru deposits similarly on the sites responsible for the hydrogen peaks. The magnitude of the reduction peak at 0.25 V, however, does not decrease in the same fashion. This is probably due to a contribution from reduction of Ru-oxide in this potential region. In fact, irreversibility in oxide formation removal has been found on Ru [20] and ruthenized electrodes [21] which supports this explanation. The current increase in the charging region is also clearly dependent on the deposition time. The irreversibility in Ru-oxide formation/removal is also noted here; irreversibility is more pronounced for the carbon-supported Pt than for smooth Pt electrodes [15]. Oxide formation on Ru electrodes is rather complex, especially after polarization to higher potential values [21–23], but, if the potential is swept up to only 0.6 V and care is taken to allow time for oxide film reduction at the hydrogen evolution edge, no oxide film build up should be possible [22]. Thus, during these Ru-deposition experiments the potential was only once swept to 0.6 V in order to obtain the CVs in Fig. 2.

The two effects of Ru-deposition mentioned above, that is decrease in hydrogen activity taken as a positive charge, Δq_H and increase in the current in the charging region Δi_{ox}, are clearly related and both could give an indication of the amount of Ru that has been deposited. In order to establish which pertained, the increase in Δq_H obtained by subtraction of the integrated voltammetric currents between 0.05 and 0.275 V from the corresponding charge for the non-modified ink, was, therefore, plotted against Δi_{ox} at 0.6 V; the result is shown in Fig. 3 together with data for smooth polycrystalline Pt. The charge and current values have been related to the real surface area of the Pt in the ink and the smooth Pt electrode. Data for the ink (triangles) lies clearly below that for polycrystalline Pt (squares). This indicates that Ru deposited on ink electrodes does not block Pt sites as effectively as when smooth Pt is used. Very little data is available on the electrochemical behaviour of Ru submonolayers on Pt. The properties of such submonolayers may be different from those of oxide layers on bulk Ru electrodes, which calls for some caution in directly applying information obtained for such electrodes to this system. Only Szabo and Bakos [24] seem to have investigated Ru submonolayers on Pt. In their study in H_2SO_4 electrolyte, they used platinized Pt electrodes and investigated, among other things, the influence of deposition potential on the voltammetry. They found that Ru, deposited in the range $0-0.2$ V (RHE), behaved similarly and that deposition above 0.5 V produced new voltammetric features, indicating a change in the oxidation state of the deposited Ru. In this experiment, wherein deposition was made at 0.1 V, the increase in the charging region should also represent the first stages of oxygen adsorption. The adspecies responsible for the Δi_{ox} are produced between 0.4 and 0.6 V and would be of the type $Ru(OH)_2$ but not that of higher oxides such as Ru_2O_3 ($E^\circ = 0.738$ V) or RuO_2 ($E^\circ = 0.937$ V) [22,24]. Returning to the data in Fig. 3, it may be noticed that linear behaviour is exhibited for Δq_H vs. Δi_{ox} for smooth polycrystalline Pt. The behaviour is an indication of a linear blocking of hydrogen adsorption sites by the deposited Ru, i.e., it seems probable that Ru is preferentially deposited on Pt rather than on itself during the electrore-

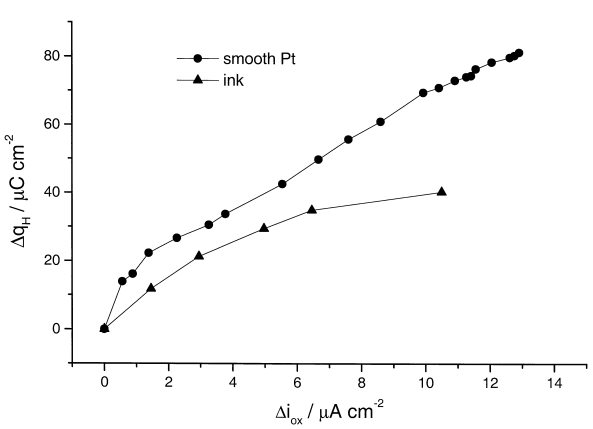

Fig. 3. Loss in hydrogen desorption charge (Δq_H) taken between 0.05 and 0.275 V as a function of increase in the oxidation current (Δi_{ox}) at 0.6 V for smooth Pt (circles) and pure ink electrode (triangles). Current and charge density is given with respect to the real surface area.

duction, at least when present in low coverages. If it is assumed that every deposited Ru adatom is oxidized in the same fashion during the positive sweep up to 0.6 V, Δi_{ox} would be a measure of the amount of surface Ru on the electrode and, for smooth Pt only, Ru attached to Pt would be present. For the ink, a slower increase in Δq_H is apparent as more Ru is deposited. The reason for this could be that Ru, in this case, is deposited differently onto the Pt crystallites, for example, in clusters in contact with the Pt, or that, in addition to deposition on Pt, some deposition straight onto carbon or in the Nafion matrix takes place. Szabo and Bakos [24] found that, for platinized Pt, some Pt hydrogen activity was always present even after deposition of visible amounts of Ru. One explanation they gave was that the Ru was deposited in the form of three-dimensional clusters in the outer layer of the platinum black substrate. A similar effect could be present for the ink electrode, too. Despite the likely inhomogeneous character of Ru deposits in the ink, the CO-tolerance was greatly improved, as will be shown below. The data in Fig. 3 can be used to estimate the distribution of Ru in the ink, as will be discussed in Section 4.2, below. In the same way, as for smooth Pt [15], the electrodeposited Ru could be removed by repetitive potential cycling (six sweeps or more) up to 1.5 V.

4. Oxidation of adsorbed CO

The CO-tolerance of fuel cell anodes is still poor because of the build up of large coverages of CO on the Pt catalyst which reduces the fuel oxidation rate. One way to study CO-tolerance to which the present flow system lends itself, is to expose the ink electrode to electrolyte which contains dissolved CO for different periods of time. After such an exposure, in the form of a short application, adsorbed CO was stripped off in pure electrolyte by a positive going potential sweep. In these experiments, CO was dosed from 5 to 90 s at 0.2 V using H_2SO_4 electrolyte in which CO was dissolved. The CO stripping voltammograms were then recorded at a sweep rate of 0.05 V s^{-1} after each application. In the following, the effect of Ru and Nafion modification of the ink is presented in addition to the data obtained using pure, unmodified ink.

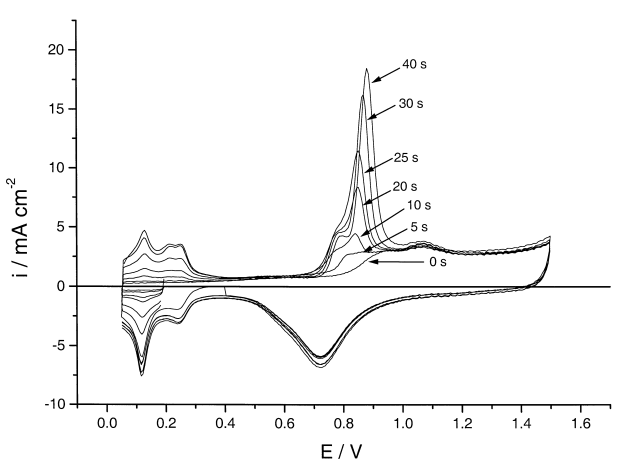

Fig. 4. CO stripping voltammetry for pure catalyst ink electrode in 0.5 M H_2SO_4 for submono and saturation adlayers created by dosing of CO containing electrolyte for various periods of time. CO was dosed at 0.2 V and the scan rate was 0.05 V s^{-1}.

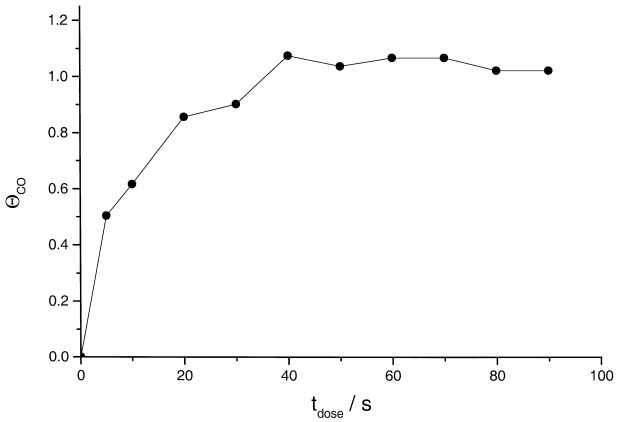

Fig. 5. CO coverage, Θ_{CO}, on the pure ink electrode as a function of dosing time. Data obtained from voltammograms is partly shown in Fig. 4.

4.1. CO stripping on ink electrode

Fig. 4 shows CVs of CO adlayers on pure ink. After dosing at 0.2 V, the potential was swept in the negative direction to the lower potential limit (0.05 V) after which an extended CV up to 1.5 V was recorded. The effect of the dosing is seen as a loss in the hydrogen sorption activity and as CO-oxidation peaks of increasing size in the range 0.7–1.0 V. The CO surface coverage, Θ_{CO}, after each increment was determined according to $\Theta_{CO} = (1/2\ \Delta q_{CO})/q_H$, where q_H is the charge under the hydrogen adsorption peaks in the negative-going sweep after stripping CO, and Δq_{CO} is the difference in the charges calculated between 0.4 and 1.5 V on the positive and negative-going sweeps, respectively; it was assumed that subtracting the oxide reduction charge on the return scan accurately compensates for the Pt surface oxide formation charge on the positive stripping sweep. The CO coverage, Θ_{CO} vs. CO dosing time is plotted in Fig. 5. As can be seen, after 40 s increment, the Pt surface is practically saturated with CO with a corresponding $\Theta_{CO} \approx 1.1$. This Faradaic coverage value is somewhat higher than that obtained for Pt(111) in H_2SO_4 electrolyte [25] ($\Theta_{CO} = 0.9$), and on similar ink in RDE experiments by Schmidt et al. [8] ($\Theta_{CO} = 0.94$).

Several CO-oxidation processes can be distinguished at ca. 0.79 and 0.85 − 0.88 V in Fig. 4. The high potential peaks actually represent the same oxidation process that is

continuously shifted in the positive direction as the coverage increases. The first process at 0.79 V, however, remains in place. It would be of interest to try to assign the CO-oxidation process to different types of adsorption sites for the molecule since the hydrogen voltammetry clearly indicates the presence of such sites. The above-mentioned coverage-dependent peak has the very same behaviour as the one found for CO on Pt(111) single crystals. For CO on Pt(111), two main oxidation peaks are found, one minor and stationary at intermediate coverages, and one that shifts to higher potentials as a function of increasing CO coverage [13,26]. The potential values are 0.75 V for the stationary and 0.83–0.88 V for the shifting peak. These values for Pt(111) are very close to those found for the ink. The stationary peak, however, disappears at saturation coverage for the Pt(111) electrode, which is not the case for the ink. In fact, for the ink, the 0.75 V peak is still present even after adding twice the amount of CO needed for a saturation layer. The stationary low potential peak for the ink may be assigned to (110) sites on the crystallite; for saturated adlayers of CO on Pt(110) a single oxidation peak at 0.75 V is found [27]. Another possibility would be that the peak is due to the oxidation of CO on edge sites on Pt(111) planes on the crystallite. CO adsorbed on such edge sites would then behave similarly to CO present in loosely packed submonolayers on Pt(111) electrodes, that is becomes oxidized at a lower potential, even though the ink has been saturated with CO.

4.2. CO stripping on ink electrode modified with Ru

This experiment was carried out in the same manner as described in Section 4.1. The difference though, was that the electrode used was the one that previously had been Ru-treated (see Section 3.2). The same effects of the CO dosing as for pure ink can be noted in Fig. 6. The CO-oxidation peaks, however, have different shapes and

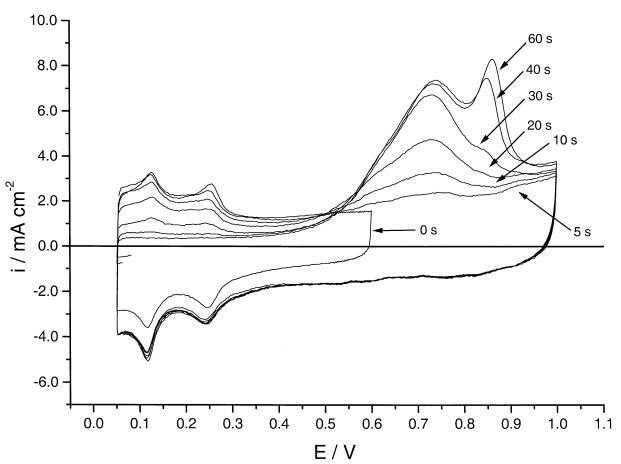

Fig. 6. CO stripping voltammetry of ink electrode modified with Ru (180 s total deposition time, basic voltammetry shown in Fig. 2) in 0.5 M H_2SO_4 at a scan rate of 0.05 V s^{-1} after CO doses of various duration.

two main peaks can be observed at 0.73 and 0.85 V. The CO-oxidation also starts at a more negative potential than on pure ink. The apparent CO saturation coverage was, calculated to be ca. 1.1, neglected here that Ru most likely has created additional adsorption sites. The high potential peak is sharp, while the low potential peak is broad and may contain contributions from several processes. After deposition, Ru is likely to be present in the ink in several forms. At first, some of it is present on or close to the Pt crystallites and some may have been deposited on the carbon support or in the Nafion film. Especially, Pt crystallites deeper inside the ink may be totally unaffected by the Ru treatment. It is possible to estimate the amount deposited on Pt crystallites and the amount deposited in the rest of the ink from the data shown in Fig. 3. It can be assumed that Δi_{ox} is a measure of the total amount of Ru which has been deposited, and also that all the Ru deposits in thin layers so that all Ru atoms contribute equally to Δi_{ox}. The amount of Ru deposited on Pt can be obtained from $m_{Ru} = (\Delta q_H d_{Pt} M_{Ru})/(q_H(tot) N_A)$, where d_{Pt} is the density of Pt surface atoms, M_{Ru} is the atomic weight of Ru, $q_H(tot)$ is the total hydrogen desorption charge for unmodified ink, N_A is the Avogadro's number, and Δq_H is obtained from Fig. 3. It is simply assumed that one Ru adatom covers one Pt surface atom when adsorbed. For the 180 s deposition on ink, $\Delta i_{ox} = 10.4$ μA cm^{-2}, which gives $\Delta q_H = 40$ μC cm^{-2} and $m_{Ru} \approx 40$ ng cm^{-2} which, in turn, amounts to an average Θ_{Ru} of 0.2.

The amount of Ru not deposited on Pt is obtained from the difference in Δq_H for the ink and smooth Pt. In this case, for the 180 s deposition, a difference in Δq_H of ca. 30 μC cm^{-2} is found. This gives, by analogous calculation, a mass of 30 ng cm^{-2} for Ru deposited on carbon or in the Nafion matrix. Thus, Ru is present in the ink both separately and in direct contact with Pt. The unaffected Pt crystallites deeper inside the film could also adsorb CO and may be the cause of the high potential peak (0.85 V) in the voltammogram in Fig. 6. The potential of these peaks is the same as that of CO oxidized on pure ink.

The remaining broad peak (0.73 V) may be attributed to CO adsorbed on the remaining sites, that is Ru/Pt and pure Ru. Peak potentials for CO-oxidation on Ru/Pt electrodes as saturated adlayers found in the literature vary between ca. 0.5 and 0.75 V depending on electrode type and composition [28–31]. For the most part, 0.5–0.6 V peaks predominate. Data obtained by Davies et al. [28] show oxidation peaks at 0.72 V for CO on some Pt(110) electrodes prepared by Ru metal vapor deposition. These electrodes had not been annealed and, thus, incorporation of the Ru adlayer into the substrate Pt lattice had not taken place. This situation might be similar to that of the present electrode and the shapes of the broad CO peaks. In fact, the Pt(110) surface exhibits the highest activity towards electrosorption of Ru among the basal planes of Pt [16]. Thus, for the ink, Ru may also be preferentially deposited on crystallite sites of (110) character. The effect of Ru

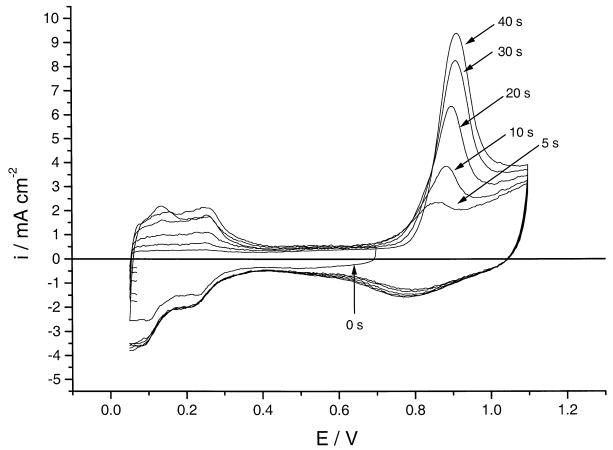

Fig. 7. CO stripping voltammetry of ink electrode covered with a Nafion film in 0.5 M H_2SO_4 at 0.05 V s^{-1} after exposure to CO doses of various duration.

modification on CO-oxidation can also be seen at lower potentials that is already at 0.4 V, a small increase in oxidation current is visible. Due to the inhomogeneous character of the Ru deposited on the ink, it is not possible to assign this enhancement effect to a particular Ru coverage or adsorption site. The electrodeposited Ru is likely to exist in a variety of local coverages and some sections of the ink may be more active towards CO-oxidation at this low potential than the sections where the main part of the CO-oxidation takes place.

4.3. CO stripping on ink electrode covered with Nafion

In Fig. 7, the CO stripping voltammetry on the ink electrode covered with a Nafion film is plotted. The situation is similar to that of the experiments in Section 4.1 except that a Nafion film of the same thickness as the ink was spin-coated on top of the ink. When Nafion is present, only one oxidation process in the form of increasing CO-oxidation peaks can be observed with peak potentials between 0.85 and 0.91 V. The maximum CO coverage was determined to be 1.3. This saturation coverage was also obtained after a 40 s CO increment, similarly to dosings made on pure ink. The higher value of Θ_{CO} for this electrode indicates that either the hydrogen adsorption is less in pure ink or more CO is present in the ink. The peak shape for CO-oxidation is, however, similar to that for pure ink and cannot be clearly assigned to any current response to non-adsorbed CO, which would be expected if additional CO were present in the ink. The question of the reason for the higher Θ_{CO} thus, remains open. The prepeak seen for CO-oxidation on the pure ink electrode is absent. One explanation for this would be that the additional Nafion polymer interacts and deactivates the proposed low coordination Pt adsorption sites responsible for the prepeak at 0.75 V. Schmidt et al. [8] also obtained a single CO-oxidation peak for saturated adlayers on their supported catalyst/Nafion electrode. The CO-oxidation peaks in Fig. 7 are shifted somewhat to higher potentials compared to the pure ink. This is most likely due to an additional IR potential drop in the Nafion film.

4.4. CO stripping on an ink electrode modified with Ru and a Nafion film

In this experiment, Ru was deposited at 0.1 V in a single step for 90 s, after which a Nafion film was spin-coated on top of it. The CO-oxidation voltammograms are shown in Fig. 8. The general behaviour of this electrode is very similar to that of the Nafion free film, Ru modified electrode (Fig. 6). One effect of the Nafion is evident however, in that the size of the lower potential peak is reduced. This is likely to be the result of deactivation of CO adsorption sites on Ru and Ru/Pt in the outer layer of the ink by the Nafion polymer. The calculated CO coverage, as if all CO were adsorbed on Pt, equals 1.5,

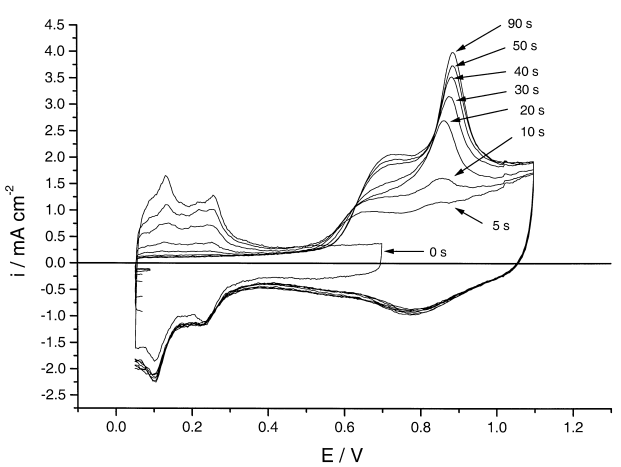

Fig. 8. CO stripping voltammetry of ink electrode modified with Ru and covered with a Nafion film in 0.5 M H_2SO_4 at a scan rate of 0.05 V s^{-1} after CO doses of various duration.

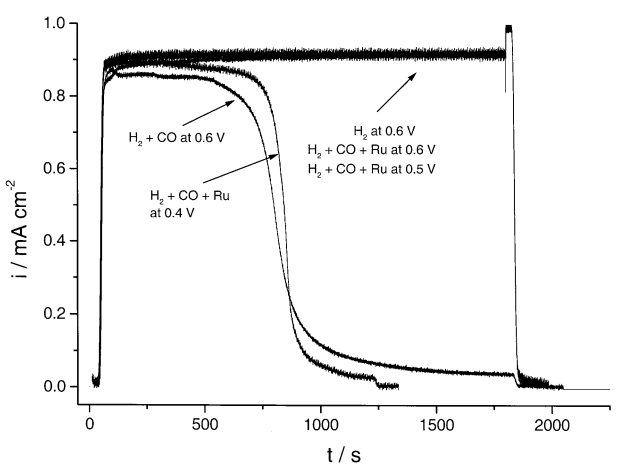

Fig. 9. Effect of electrodeposited Ru on CO tolerance in amperometric oxidation of H_2 and CO containing H_2SO_4 electrolyte. CO concentration in electrolyte sparging gas: 1.4% by volume.

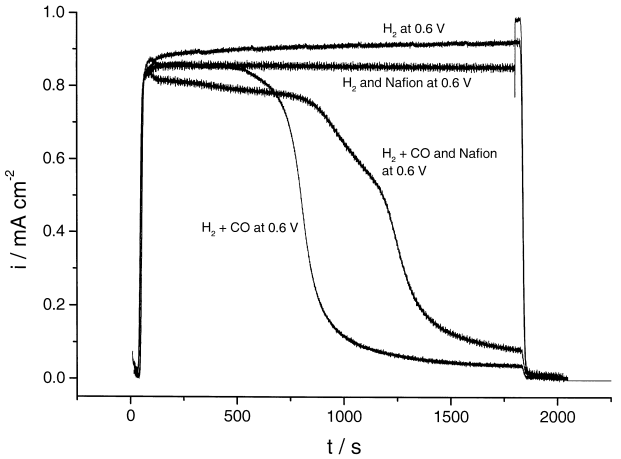

Fig. 10. Effect of Nafion film deposited on top of catalyst ink on amperometric oxidation of H_2 and CO containing H_2SO_4 electrolyte. CO concentration in electrolyte sparging gas: 1.4% by volume.

which is higher than without Nafion film. This is an indication that the Nafion polymer, indeed, may play a role as a storage site for non-adsorbed CO.

5. Continuous oxidation of H_2 and H_2 + CO containing electrolyte

The amperometric measurements were carried out by means of flows of H_2SO_4 electrolyte solutions saturated with H_2 or with H_2 + 1.4% CO (v/v). Two different experiments were performed. First, the influence of electrodeposited Ru, 90 s, single application, on the CO-tolerance was investigated and the results are shown in Fig. 9. At 0.6 V polarization, the pure ink electrode is poisoned quite rapidly, that is, after ca. 750 s. When the measurement was repeated after Ru modification, no CO poisoning was found during the 0.5 h measurement. Decreasing the potential to 0.5 V did not alter the situation. However, when the potential was further decreased to 0.4 V, poisoning set in at about 800 s.

In the second experiment, a Nafion film was spin-coated on top of the ink and the resulting amperometry data are shown in Fig. 10. For a pure H_2 electrolyte flow at 0.6 V, the Nafion film somewhat reduces the oxidation rate (ca. 5%), but the Nafion film clearly improved the CO-tolerance. Interestingly, the Nafion film introduces a new linear section in the amperometric curve. The curve for non-Nafion modified ink is shown for reference.

The results from these amperometric experiments show that the flowing electrolyte system allows easy comparison of oxidation rates for differently treated ink electrodes. The CO concentration in the H_2-containing electrolyte used was much higher than was expected to be encountered in a fuel cell anode operating on reformed hydrogen. However, these measurements were undertaken only to demonstrate the feasibility of this flow system; the CO concentration could easily be lowered, if needed.

The hydrodynamics of the wall-jet electrode used in this work is such that the center of the electrode has a somewhat better access to reactants compared to the edges [32]. This may complicate interpretation of the kinetics of the fuel oxidation reaction. However, the validity of a direct comparison of the rates for differently treated thin film electrodes in the same flow cell should be justified.

6. Conclusions

The flow system has been shown to be suitable for testing fuel cell electrode material in the form of thin films of catalyst ink or ink covered by additional Nafion film. The CO-tolerance can be rapidly tested, either by creating controlled adlayers of CO or by continuous oxidation of CO containing H_2-electrolyte. In both cases, a CO-free electrode environment is obtained a few seconds after selecting pure electrolyte flow. This is clearly much more convenient than having to sparge a cell with static electrolyte saturated with inert gas after exposure to CO. In situ electrochemical Ru modification of the ink electrode has been demonstrated and the electrochemistry of adlayers of Ru has been interpreted and compared to the data for smooth Pt electrodes. Rapid testing of the effects of deposited Ru on CO-tolerance has also been demonstrated, both for dosed CO adlayers and during continuous oxidation of hydrogen. The ink electrodes covered with Nafion showed a lower rate of H_2 oxidation due to the reduced mass transport rate, but the Nafion film reduced the CO poisoning rate in amperometric measurements on ink not modified by Ru. Clearly, in this report, only few examples of the use of the flow cell approach were demonstrated and no in depth analysis of specific fuel cell problems were attempted. However, confidence is felt that the method has a capability for rapid screening of different inks in thin film form and, also, that the systematic study of in situ metal adatom modification effects are possible.

Acknowledgements

The support of the Neste foundation and the Finnish Technology Development Centre is gratefully acknowledged.

References

[1] P.S. Kauranen, E. Skou, J. Munk, J. Electroanal. Chem. 404 (1996) 1.
[2] T.R. Ralph, G.A. Hards, J.E. Keating, S.A. Campbell, D.P. Wilkinson, M. Davis, J. Stpierre, M.C. Johnson, J. Electrochem. Soc. 144 (1997) 3845.
[3] K.H. Choi, H.S. Kim, H.L. Tae, J. Power Sources 75 (1998) 230.

[4] T.J. Schmidt, H.A. Gasteiger, R.J. Behm, Electrochem. Commun. 1 (1999) 1.
[5] E. Antolini, L. Giorgi, A. Pozio, E. Passalacqua, J. Power Sources 77 (1999) 136.
[6] V.N. Fateev, E.K. Lyutikova, R. Amadelli, Russ. J. Electrochem. 35 (1999) 183.
[7] G. Tamizhmani, J.P. Dodelet, D. Guay, J. Electrochem. Soc. 143 (1996) 18.
[8] T.J. Schmidt, H.A. Gasteiger, G.D. Stäb, P.M. Urban, D.M. Kolb, R.J. Behm, J. Electrochem. Soc. 145 (1998) 2354.
[9] J.M. Rheaume, B. Mueller, M. Schulze, J. Power Sources 76 (1998) 60.
[10] M. Wasberg, J. Electroanal. Chem. 379 (1994) 541.
[11] M. Wasberg, G. Horanyi, J. Electroanal. Chem. 381 (1995) 151.
[12] M. Bergelin, M. Wasberg, J. Electroanal. Chem. 449 (1998) 181.
[13] M. Bergelin, J.M. Feliu, M. Wasberg, Electrochim. Acta 44 (1997) 1069.
[14] M. Bergelin, E. Herrero, J.M. Feliu, M. Wasberg, J. Electroanal. Chem. 467 (1999) 74.
[15] U. Koponen, M. Bergelin, J.M. Feliu, M. Wasberg, manuscript in preparation.
[16] U. Koponen, M. Bergelin, J.M. Feliu, M. Wasberg, manuscript in preparation.
[17] G.J.K. Acres, J.C. Frost, G.A. Hards, R.J. Potter, T.R. Ralph, D. Thompsett, G.T. Burstein, G.J. Hutchings, Catal. Today 38 (1997) 393.
[18] S. Wasmus, A. Kuver, J. Electroanal.Chem. 461 (1999) 14.
[19] C.M. Brett, A.M. Oliveira Brett, Hydrodynamic electrodes, in: Electrode Kinetics: Principles and Methodology, C.H. Bamford, R.G. Compton (Eds.), Compr. Chem. Kinet. 5 Elsevier, Amsterdam, 1986, pp. 355–434.
[20] R.C. Walker, M. Bailes, L.M. Peter, Electrochim. Acta 44 (1998) 1289.
[21] B.E. Conway, H. Angerstein-Kozlowska, M. Vukovic, S. Hadzi-Jordanov, J. Phys. Chem. 81 (1977) 2271.
[22] R.O. Lezna, N.R. Detacconi, A. Arvia, J. Electroanal. Chem. 151 (1983) 193.
[23] V. Birss, R. Myers, H. Angerstein-Kozlowska, B.E. Conway, J. Electrochem. Soc. 131 (1984) 1502.
[24] S. Szabo, I. Bakos, J. Electroanal. Chem. 230 (1987) 233.
[25] M.J. Weaver, S.-C. Chang, L.-W.H. Leung, X. Jiang, M. Rubel, M. Szklarczyk, D. Zurawski, A. Wieckowski, J. Electroanal. Chem. 327 (1992) 247.
[26] M. Bergelin, Feliu, unpublished results.
[27] B.E. Hayden, A.J. Murray, R. Parsons, D.J. Pegg, J. Electroanal. Chem. 409 (1996) 51.
[28] J.C. Davies, B.E. Hayden, D.J. Pegg, Electrochim. Acta 44 (1998) 1181.
[29] A. Kabbabi, R. Faure, D. Durand, B. Beden, F. Hahn, J.M. Leger, C. Lamy, J. Electroanal. Chem. 444 (1998) 41.
[30] T.J. Schmidt, M. Noeske, H.A. Gasteiger, R.J. Behm, P. Britz, W. Brijoux, H. Bonnemann, Langmuir 13 (1997) 2591.
[31] Y. Morimoto, E. Yeager, J. Electroanal. Chem. 441 (1998) 77.
[32] K.B. Prater, A.J. Bard, J. Electrochem. Soc. 117 (1970) 207.